Simplified Electromagnetic Modelling of Accelerator Magnets Wound with Conductor on Round Core Wires for AC Loss Calculations

Yusuke Sogabe, *Member, IEEE,* Masahiro Yasunaga, and Naoyuki Amemiya, *Member, IEEE*

***Abstract*—We developed a simplified three-dimensional electromagnetic field analysis model for accelerator magnets wound with Conductor on Round Core (CORC®) to estimate ac loss of magnets. In our model, the coil winding of the analyzed magnet was separated into several divisions composed of dozens of turns. Then, ac loss density in a division was assumed to be the same as that of a single CORC® wire exposed to magnetic field in a representative turn of the division. We carried out the ac loss calculations using the model for a superferric magnet composed of coil wound with CORC® wires and iron core.**

***Index Terms*—AC loss, accelerator magnet, conductor on round core wires, electromagnetic field analysis, rapid-cycling synchrotron**

I. Introduction

CONDUCTOR on round core (CORC®, written here as just "CORC") wires are attractive assembled conductors for applications to accelerator magnets because of their large current capacity and mechanical flexibility [1]–[6]. Because accelerator magnets are sometimes employed to generate time-dependent magnetic fields, ac losses and their distribution in the magnets can be an issue due to thermal runaway and burn out of coil windings [7]–[10]. Electromagnetic field analysis is a convenient tool for ac loss calculation of CORC wires composing accelerator magnets. However, electromagnetic field analyses of accelerator magnets wound with CORC wires are difficult because of the complicated three-dimensional geometry of the coated conductors in CORC wires. In CORC wires, the overlapping of coated conductors is not uniform along the cable axis. Therefore, there are some places in CORC wires where the magnetic flux can penetrate into coated conductors easily. As a consequence, the ac loss density distribution is not uniform along the wire axis. Therefore, to accurately estimate the ac losses of CORC wires, three-dimensional simulations are necessary.

Manuscript receipt and acceptance dates will be inserted here. This work was supported in part by the Ministry of Education, Culture, Sports, Science and Technology under the Innovative Nuclear Research and Development Program. *(Corresponding author: Naoyuki Amemiya.)*

Y. Sogabe, M. Yasunaga, and N. Amemiya are with the Department of Electrical Engineering, Kyoto University, Kyoto 615-8510, Japan (e-mail: amemiya.naoyuki.6a@kyoto-u.ac.jp).

Color versions of one or more of the figures in this paper are available online at http://ieeexplore.ieee.org.

Digital Object Identifier will be inserted here upon acceptance.

In this paper, we report a simple electromagnetic field analysis model for ac loss calculations of accelerator magnets wound with CORC wires. In the model, a representative CORC wire in a coil winding is approximated by a single CORC wire that is exposed to the magnetic field where the representing CORC wire is placed in the coil winding. We designed a superferric magnet composed of coil wound with CORC wires and iron core for a rapid-cycling synchrotron to compute the ac loss in the magnet. The AC loss distributions in coated conductors composing a CORC wire representing one turn of the coil winding are calculated and discussed based on the calculated magnetic field in the cross-sections of the CORC wire.

II. Simplified Electromagnetic Modeling of Magnets Wound with CORC Wires

A. Modeling Overview

To calculate ac losses in accelerator magnets wound with CORC wires, we need to construct a simplified electromagnetic field analysis model. The three-dimensional geometry of the coated conductor composing the CORC wires is important for their ac loss characteristics. In addition, the complicated distributions of the magnetic field seen by the coated conductors composing CORC wires in the magnets are also the key for the ac loss characteristics of the CORC wires wound into the coils. Therefore, it is important in the modeling to be able to consider the three-dimensional geometry of the CORC wires and the three-dimensional magnetic field distribution in the coated conductors composing CORC wires.

First, two-dimensional magnetic field distribution in a cross-section of a CORC wire that corresponds to one turn of the coils is calculated based on static field calculation. In the case of magnets including iron yokes, the non-linear magnetic flux density B–magnetic field H should be considered. Second, the calculated two-dimensional magnetic field distribution in the cross-section of the CORC wire is assumed uniform along the longitudinal direction of the CORC wire. Finally, a three-dimensional electromagnetic field analysis is conducted for the CORC wire, and the ac loss density at the typical point is calculated from the ac loss calculation result of the CORC wire.

In the model because the three-dimensional geometry of coil windings is simplified as a single straight CORC wire, the in-

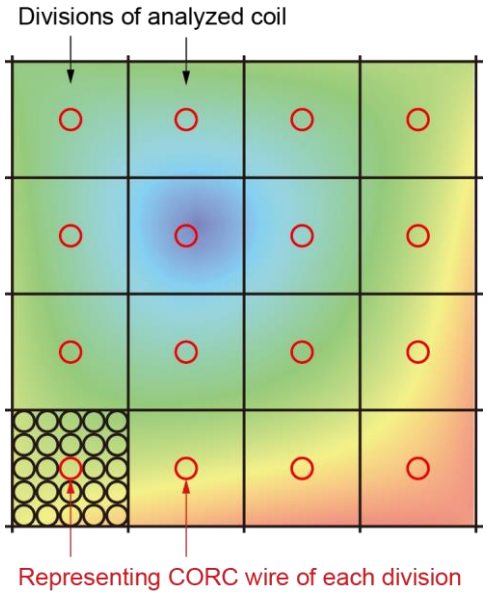

Fig. 1. Schematics of a coil wound with CORC wires divided into some divisions and representing CORC wires of the divisions. In this schematics, magnitude of magnetic flux density in the coil is shown with color.

fluence of the curved geometry of the coil windings is ignored. Furthermore, the strict current distribution in the CORC wires is neglected, and uniform current density distribution in the coil cross-section is assumed. Moreover, the nonuniform current density distribution influenced by induced shielding currents in the coated conductors composing the non-analyzed CORC wires is not considered. These ignored components are not dominant for the results of ac loss calculation in the CORC wire. Because the CORC wire is part of a large-scale accelerator magnet that has a large number of turns, the current that generates an external magnetic flux density and the magnetized iron yoke are much higher than them.

B. Calculation of Magnetic Field in a CORC Wire in Coil Winding

In the model, some cross-sections of coil windings are chosen. Then, each is separated into divisions composed of dozens of CORC wires. AC loss density is approximated in a cross-section division within one CORC wire corresponding to the representing turn as shown in Fig. 1 (in this paper, the representing turn is defined as the central turn of the division). To calculate the ac loss density in the representative CORC wire, we assume that the magnetic flux density observed by every CORC wire in each division has the same distribution in a cross-section of the representative CORC wire. Moreover, we assume that the magnetic flux density distribution along the coil winding direction is uniform. Therefore, the ac loss density in a division is approximated by the ac loss density in a single infinitely long straight CORC wire that is exposed to a two-dimensional magnetic flux density in the cross-section of the representing CORC wire of the division.

Another possible modelling of magnetic field distribution in an analyzed CORC wire in coil windings is calculating three-dimensional field distribution in the coated conductors for one-

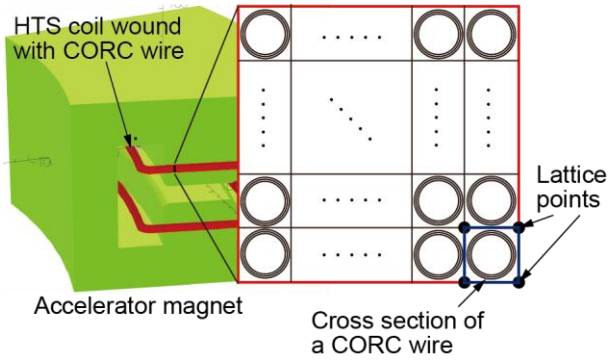

Fig. 2. Schematics of a cross-section of HTS coils wound with CORC wires composing an accelerator magnet. The cross-section of the coils are divided into a lattice, and magnetic flux density distribution is calculated on the lattice points. Each section of lattice corresponds one turn (one CORC wire).

pitch length. The difference between these modelling is whether we consider non-uniform magnetic field distribution along the cable axis in final three-dimensional simulation for ac loss calculation. By the latter modelling, magnetic field at one end of a section of a CORC wire is not congruent with it at the other end. Therefore, we cannot consider periodic boundary for the section of the CORC wire. It causes problem in the simulation of the CORC wire assumed having infinite length. Although three-dimensional simulation of the section of a CORC wire is one of other choices, the ac loss density distribution could be different because the long length in the coil winding is not considered. Consequently, we use former modelling.

The calculation procedure to obtain the magnetic flux density in a representative CORC wire of a division is as follows. First, the magnetic flux density seen by the cross-section of a CORC wire is calculated, which corresponds to a representing turn of a division of the analyzed coil. In this approximation, instead of exact current distributions in the CORC wires composing the coil winding, the uniform current density in the cross-section of the coil winding is assumed, and two-dimensional magnetic flux density is calculated on the lattice points shown in Fig. 2. Here, each section of the lattice corresponds to one turn (one CORC wire). By using the magnetic flux density on the lattice points of the analyzed CORC wire, the two-dimensional magnetic flux density is calculated in the analyzed CORC wire by using linear interpolation.

Second, the three-dimensional magnetic flux density distribution is calculated in the coated conductors composing the single straight CORC wire by using the calculated two-dimensional magnetic flux density distribution in the CORC wire. Here, the calculated magnetic flux density distribution in the cross-section of the CORC wire is assumed to be uniform along the longitudinal direction of the CORC wire. We refer to the calculated three-dimensional magnetic flux density as the external magnetic field. Because the three-dimensional geometry of the coated conductors composing the CORC wire is considered in the model, the magnetic flux density distribution seen by the coated conductors is not uniform along the longitudinal direction of the coated conductors even if the CORC wire is under two-dimensional magnetic flux density distribution.

C. Three-Dimensional Electromagnetic Field Analysis of a Single CORC Wire

To calculate the ac loss in a single infinite-long CORC wire exposed to an external magnetic field, we conducted three-dimensional electromagnetic field analysis. The equation is derived from Faraday's law, Biot–Savarts law, Ohm's law, and the definition of the current vector potential. In addition, the thin-strip approximation is used in the model for coated conductors. The governing equation is as follows [11]:

$$\nabla\times\left(\frac{1}{\sigma}\nabla\times\boldsymbol{n}T\right)\cdot\boldsymbol{n}+\frac{\partial}{\partial t}\frac{\mu_0 t_s}{4\pi}\cdot\left(\int_{S'}\left[\left\{(\nabla\times\boldsymbol{n}'T')\times\boldsymbol{r}\cdot\boldsymbol{n}\right\}/r^3\right]\mathrm{d}S'+\boldsymbol{B}_{\mathrm{ext}}\cdot\boldsymbol{n}\right)=0. \quad (1)$$

Here, T and T' are the magnitudes of the current vector potentials at the field point where the potential is calculated and the source point where the current exists, respectively. $\boldsymbol{n}$ and $\boldsymbol{n}'$ are normal vectors at the field point and source points, respectively, and $\boldsymbol{r}$ is a vector from the source point to the field point. t_s and σ are the thickness of the superconductor layer of the coated conductor and its equivalent conductivity, respectively. $\boldsymbol{B}_{\mathrm{ext}}$ is the external magnetic flux density applied to the analyzed coated conductors. S' is the area of the wide face of the superconductor layer of the analyzed magnet.

Some accelerator magnets have iron yokes that have nonlinear magnetic flux density B–magnetic field H. To calculate ac losses in coils wound with CORC wires in this type of accelerator magnet, we need to consider the influence of the magnetized iron yoke on the magnetic flux density distribution in the coil windings. To consider this, we apply the approximation described in [10]. In the approximation, the influence of magnetized iron yokes is considered as externally applied magnetic flux density $\boldsymbol{B}_{\mathrm{ext}}$ in equation (1). Namely, we can consider the nonlinear B–H characteristics as time-dependent B_{ext}, which is not proportional to the transport current in the coils.

Furthermore, in the 3D simulation of CORC wires, the influence of magnetization of the coated conductors (the magnetic coupling) is considered in the simulation, but coupling current through finite contact resistance (the electrical coupling) is not considered. Therefore, in this simulation, we assumed a uniform transport current in each coated conductor. The validity of the electromagnetic field analysis model for single CORC wires was confirmed through a comparison between measurements and analyses [12].

III. Specifications of Designed Magnet and CORC Wires for Test Analysis

We designed a magnet composed of an iron yoke and HTS coil wound with CORC wires and calculated ac loss density in a coil division.

The analyzed magnet is designed based on requirements for a rapid cycling synchrotron [10]. The magnet is a combined-function magnet that generates dipole and quadrupole components of the magnetic field. The bird view image of the magnet is shown in Fig. 3(a), and the cross-section of the magnet is shown in Fig. 3(b). The specifications of the HTS coils and CORC wires are listed in Table I. The HTS coil composing the magnet consists of stacked curved racetrack coils. The HTS coils in the magnet are operated at 65 K in liquid nitrogen, reducing the pressure, but the iron yoke is placed in room temperature area. We assume that the HTS coils are surrounded by liquid nitrogen, heat insulation, and cryostat.

The three-dimensional geometry of the CORC wire is shown in Fig. 4. As described in Sec. II, the three-dimensional geometry of the CORC wire is essential for ac loss calculations. In the three-dimensional electromagnetic field analysis, we use the

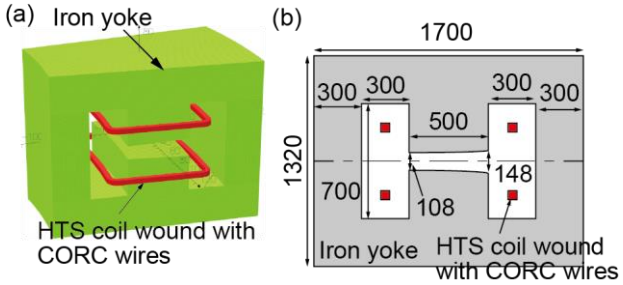

Fig. 3. Configuration of the designed and analyzed magnet which is composed of iron yoke and HTS coil wound with CORC wires; (a) Bird view of the designed magnet; (b) Cross-section of the designed magnet.

TABLE I
Specifications of the HTS coil and the CORC wires

Parameters of the HTS coil	
Number of CORC wires	400 (20 × 20)
Separation between CORC wires	0.03 mm
Maximum transport current	186 A/wire 31.0 A/tape
Frequency of current	100 Hz
Parameters of the CORC wires	
Number of layers	3
Number of coated conductors per layer	2
Diameter of core	2.5 mm
Width of tape	2.0 mm
Thickness of superconducting layer	1.0 μm
Separation between layers	45 μm
Pitch length	5.6 mm

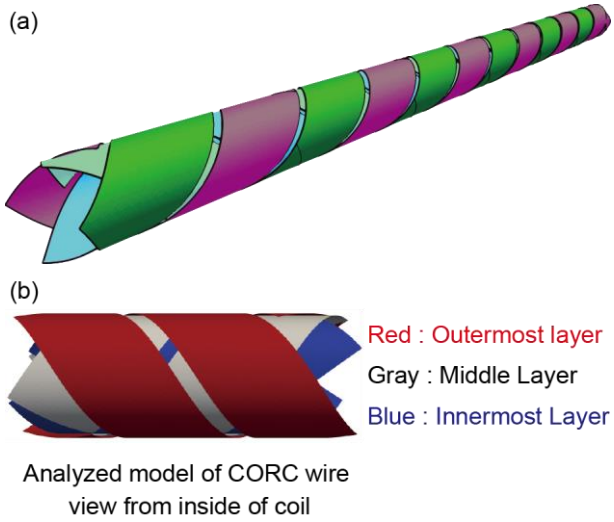

Fig. 4. Three-dimensional geometry of the CORC wire: (a) Bird view and (b) side view.

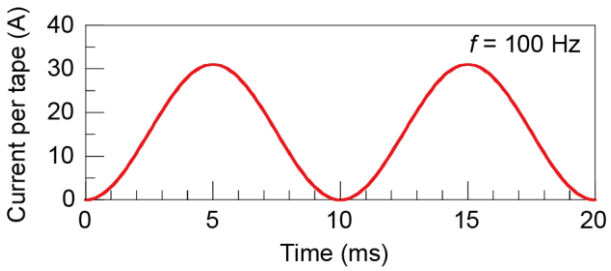

Fig. 5. Current profile of the magnet. Here, current per strand (coated conductor) in the CORC wire is plotted.

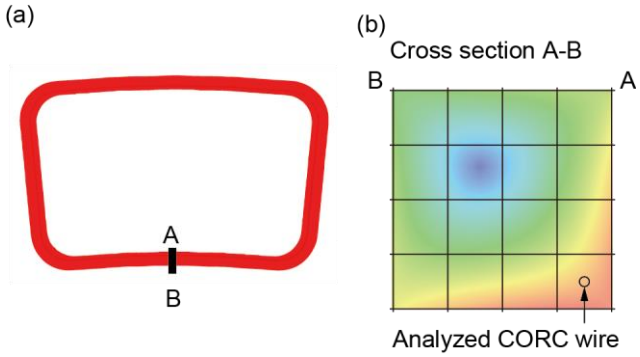

Fig. 6. Schematics at where the model is applied; (a) top view of the coil winding and analyzed coil cross-section A-B and (b) analyzed CORC wire in the coil cross-section A-B.

symmetrical geometry of the CORC wire, and then the analyzed objects are reduced to one tape of each layer.

The current profile of the HTS coils is shown in Fig. 5. Here, the current per strand (coated conductor) in the CORC wire is plotted. For the electromagnetic field analysis, we use the formulated electric field E–current density J characteristics of the coated conductors composing the CORC wire [10]. The formulation is based on the power-law model and Kim model [13] as follows:

$$E = E_0\left(\frac{J}{J_c(B,\varphi)}\right)^{n(B,\varphi)}, \tag{2}$$

where E_0 is the defining electric field criterion (fixed at 10^{-4} V/m) for the critical current density J_c. The dependence of J_c and n-value is determined based on the measured electric field–current characteristics under various external magnetic flux densities of a coated conductor at 65 K. We formulated the dependence of J_c and n-value on magnitude and angle of magnetic flux density as follows [14]:

$$x(B,\varphi) = \left(x_{ab}^{m} + x_{c}^{m}\right)^{1/m}, \tag{3}$$

$$x_{ab,c}(B,\varphi) = x_{0ab,c} \Big/ \left(1 + B f_{ab,c}(\varphi)/B_{0ab,c}\right)^{\beta_{ab,c}}. \tag{4}$$

Here, x represents either J_c or n, $x_{0ab,c}$ represents either $J_{c0ab,c}$ or $n_{0ab,c}$, and the subscript ab,c means ab or c. The angular dependence $f_{ab,c}(\varphi)$ is as follows:

$$f_{ab}(\varphi) = \sqrt{u_{ab}{}^2 \cos^2(\varphi - \delta_{ab}) + \sin^2(\varphi - \delta_{ab})}, \tag{5}$$

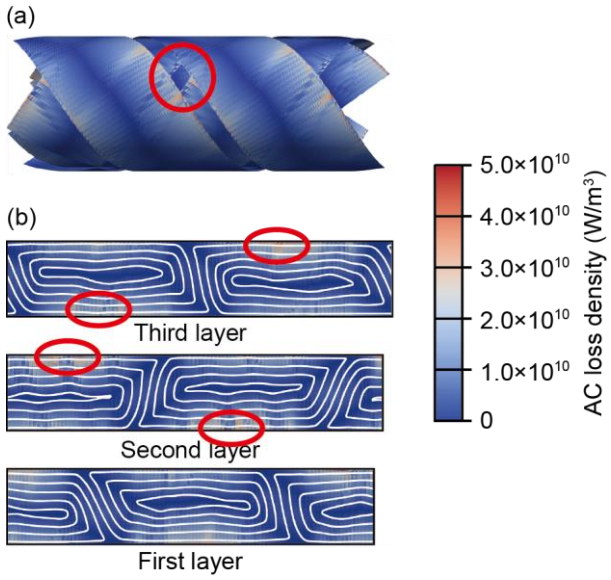

Fig. 7. Ac loss density distribution in the analyzed CORC wire at t = 15 s (when current is maximum in second cycle): (a) three-dimensional distribution in the CORC wire and (b) two-dimensional distribution in the developed coated conductor with current lines (white lines). The first layer means the coated conductor in the innermost layer of the CORC wire, and the third layer means the coated conductor in the outermost layer of CORC wire. Each coated conductor is enlarged in width direction.

$$f_c(\varphi) = \begin{cases} \sqrt{\cos^2(\varphi - \delta_c) + u_c{}^2 \sin^2(\varphi - \delta_c)} \\ \qquad (-90° + \delta_c \le \varphi \le 90° + \delta_c) \\ \sqrt{v^2 \cos^2(\varphi - \delta_c) + u_c{}^2 \sin^2(\varphi - \delta_c)} \\ \qquad (otherwise) \end{cases}. \tag{6}$$

where $\varphi = 0°$ is the direction of the normal vector to the wide face of the REBCO conductor.

IV. AC Loss Calculation Results

A. Conditions for Application of the Model

We calculate ac loss density in the division shown in Fig. 6. In this division, the magnetic flux density seen by the coated conductors composing the representing CORC wire is the largest among all divisions. Therefore, the ac loss density in the division should be the highest.

B. AC Loss Density and Current Distribution in the Analyzed CORC Wire

The calculated three-dimensional ac loss density distribution in the CORC wire at t = 15 s is shown in Fig. 7(a). The calculated ac loss density is in the superconductor layers of the coated conductors. We can see the local concentration of ac loss in the red circle. Here, there is a non-covered area by the coated conductors in the third and second layers. In this situation, the shielding effect of coated conductors against the external magnetic field is weak, and the magnetic flux can penetrate into the coated conductors from this part. This effect increases the ac loss density in the coated conductors. The ac loss density distributions in the developed coated conductors composing the

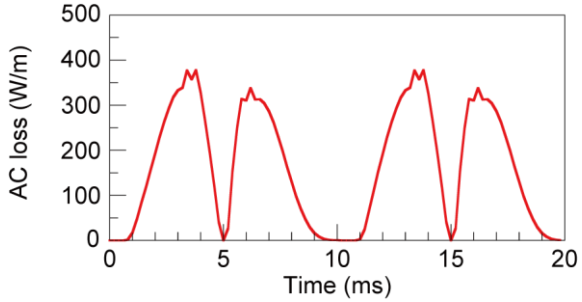

Fig. 8. Temporal changing of ac loss per length of the analyzed CORC wire.

CORC wire are shown in Fig. 7(b) with current lines. Here, the first layer is the coated conductor in the innermost layer of the CORC wire, and the third layer is the coated conductor in the outermost layer of the CORC wire. Each coated conductor is enlarged in the width direction of the coated conductor. We can see the effect of the non-covered area on the ac loss density distribution in the coated conductors. In this area, the current also concentrates on the edge of the coated conductors.

Moreover, the loops of the shielding currents induced by the external magnetic field are closed in the half-pitch of the CORC wire. This is because of the three-dimensional spiral geometry of the coated conductor in the CORC wire. In this geometry, the normal component of magnetic field seen by the coated conductors in the CORC wire is altered in half-pitch of the CORC wire.

C. Temporal Evolution of AC Loss in the Analyzed CORC Wire

The calculated temporal change in ac loss per length of the analyzed CORC wire is shown in Fig. 8. Here, the calculated ac loss denotes the overall ac loss of all coated conductors composing the analyzed CORC wire. We can see the ac loss becomes zero at t = 5 ms and t = 15 ms. Namely, the ac loss is strongly influenced by dI/dt or dB_{ext}/dt: I denote current, and B_{ext} denotes the external magnetic flux density. This is because the loops of shielding currents are closed in the half-pitch of the CORC wire as shown in Fig. 7(b), and therefore, the inductance of the loops of the shielding currents and decay time constants of them are much smaller than them in the coils wound with not-twisted single coated conductor.

V. Conclusion

A simplified electromagnetic field analysis model was developed for ac loss calculations of accelerator magnets wound with CORC wires. In the model, each turn of the coil winding composing the magnet, i.e. single CORC wire, is the analyzed object. The magnetic flux density distribution in the CORC wire is calculated based on the assumption of uniform current density in the coil cross-section. By using the model, we can calculate the three-dimensional ac loss density distribution in coated conductors composing the CORC wire. We applied the model to an accelerator magnet and calculated the ac loss in a part of coil winding. The three-dimensional geometry of the CORC wire contributed to the characteristics of the ac loss distribution in the CORC wire which was observed as local concentration of ac loss density and small inductance of shielding current loops in the coated conductors.

References

[1] D.C. van der Laan, J.D. Weiss, P. Noyes, U.P. Trociewitz, A. Godeke, D. Abraimov, and D.C. Larbalestier, "Record current density of 344 A mm^{-2} at 4.2 K and 17 T in CORC® accelerator magnet cables," *Supercond. Sci. Technol.*, vol. 29, no. 5, May 2016, Art. no. 055009.

[2] X. Wang, S. Caspi, D.R. Dietderich, W. B. Ghiorso, S.A. Gourlay, H.C. Higley, A. Lin, S.O. Prestemon, D. van der Laan, and J.D. Weiss, "A viable dipole magnet concept with REBCO CORC® wires and further development needs for high-field magnet applications," *Supercond. Sci. Technol.*, vol. 31, no. 4, Apr. 2018, Art. no. 045007.

[3] M. Vojenciak, A. Kario, B. Ringsdorf, R. Nast, D.C. van der Laan, J. Scheiter, A. Jung, B. Runtsch, F. Gomory, and W. Goldacker, "Magnetization ac loss reduction in HTS CORC® cables made of striated coated conductors," *Supercond. Sci. Technol.*, vol. 28, no. 10, Oct. 2015, Art. no. 104006.

[4] P.C. Michael, L. Bromberg, D.C. van der Laan, P. Noyes, and H.W. Weijers, "Behavior of a high-temperature superconducting conductor on a round core cable at current ramp rates as high as 67.8 kA s^{-1} in background fields of up to 19 T," *Supercond. Sci. Technol.*, vol. 29, no. 4, Apr. 2016, Art. no. 045003.

[5] T. Mulder, A. Dudarev, M. Mentink, D. van der Laan, M. Dhalle, and H. ten Kate, "Performance test of an 8 kA @ 10-T 4.2-K ReBCO-CORC cable," *IEEE Trans. Appl. Supercond.*, vol. 26, no. 4, Jun. 2016, Art. no. 4803705.

[6] C.S. Myers, M.D. Sumption, and E.W. Collings, "Magnetization and flux penetration of YBCO CORC cable segments at the injection fields of accelerator magnets," *IEEE Trans. Appl. Supercond.*, vol. 29, no. 5, Aug. 2019, Art. no. 4701105.

[7] J. van Nugteren, B. van Nugteren, P. Gao, L. Bottura, M. Dhalle, W. Goldacker, A. Kario, H. ten Kate, G. Kirby, E. Krooshoop, G. de Rijk, L. Rossi, C. Senatore, S. Wessel, K. Yagotintsev, and Y. Yang, "Measurement and numerical evaluation of AC losses in a ReBCO Roebel cable at 4.5 K," *IEEE Trans. Appl. Supercond.*, vol. 26, no. 3, Apr. 2016, Art. no. 8201407.

[8] H. Piekarz, S. Hays, Y. Huang, V. Kashikhin, G. de Rijk, and L. Rossi, "Design considerations for fast-cycling superconducting accelerator magnets of 2 T B-field generated by a transmission line conductor of up to 100 kA current," *IEEE Trans. Appl. Supercond.*, vol. 18, no. 2, Jun. 2008, pp. 256–9.

[9] Y. Sogabe and N. Amemiya, "AC loss calculation of a cosine-theta dipole magnet wound with coated conductors by 3D modeling," *IEEE Trans. Appl. Supercond.*, vol. 28, no. 4, Jun. 2018, Art. no. 8200705.

[10] Y. Sogabe, M. Yasunaga, Y. Fuwa, Y. Kuriyama, T. Uesugi, Y. Ishi, and N. Amemiya, "AC losses in HTS coils of superferric dipole and combined-function magnets for rapid-cycling synchrotrons," *IEEE Trans. Appl. Supercond.*, vol. 29, no. 5, Aug. 2019, Art. no. 5900505.

[11] Nii M, N. Amemiya, and T. Nakamura, "Three-dimensional model for numerical electromagnetic field analyses of coated superconductors and its application to Roebel cables," *Supercond. Sci. Technol.*, vol. 25, no. 9, Sep. 2012, Art. no. 095011.

[12] N. Amemiya and R. Toyomoto, "Ac loss measurements of CORC wires carrying ac transport currents and / or exposed to ac transverse magnetic fields," *2018 Applied Superconductivity Conference*, 1MOr1A-01.

[13] Y.B. Kim, C.F. Hempstead, and A.R. Strnad, "Critical persistent currents in hard superconductors," *Phys. Rev. Lett.*, vol. 9, no. 7, pp. 306–309, Oct. 1962.

[14] Y. Sogabe, Z. Jiang, S.C. Wimbush, N.M. Strickland, M. Staines, N.J. Long, and N. Amemiya, "AC loss characteristics in REBCO coil assemblies with different geometries and conductors," *IEEE Trans. Appl. Supercond.*, vol. 28, no. 3, Jun. 2015, Art. no. 4900205.